

Hypoxia evokes increased PDI and PDIA6 expression in the infarcted myocardium of ex-germ-free and conventionally-raised mice

Klytaimnistra Kiouptsi^{1*}, Stefanie Finger², Venkata S. Garlapati², Maike Knorr², Moritz Brandt^{1,2,3}, Ulrich Walter^{1,3}, Philip Wenzel^{1,2,3}, Christoph Reinhardt^{1,3*}

¹Center for Thrombosis and Hemostasis (CTH), University Medical Center Mainz, Johannes Gutenberg University Mainz, Langenbeckstrasse 1, 55131 Mainz, Germany. ²Center for Cardiology, Cardiology I, University Medical Center Mainz, 55131 Mainz, Germany. ³German Center for Cardiovascular Research (DZHK), Partner Site RheinMain, Mainz, Germany.

Keywords: HL-1 cardiomyocytes, hypoxia, left anterior artery descending ligation, P4HB, PDIA6, germ-free

The authors declare that no conflicts of interest exist.

*Corresponding authors:

Christoph Reinhardt, Christoph.Reinhardt@unimedizin-mainz.de and

Klytaimnistra Kiouptsi, emy.kiouptsi@gmail.com

Phone: +49-6131-17-8280; FAX: +49-6131-17-6238

Summary statement

We identified PDIA6 as a hypoxia-induced element of the unfolded protein response in cardiomyocytes and infarcted mouse hearts. PDIA6 expression and ejection fractions were reduced in infarcted ex-germ-free mouse hearts.

Abstract

The prototypic protein disulphide isomerase (PDI), encoded by the P4HB gene, has been described as a survival factor in ischemic cardiomyopathy. However, the role of protein disulfide isomerase associated 6 (PDIA6) under hypoxic conditions in the myocardium remains enigmatic and it is unknown whether the gut microbiota influences the expression of PDI and PDIA6 under conditions of acute myocardial infarction. Here, we revealed that in addition to the prototypic PDI, the PDI family member (PDIA6), a regulator of the unfolded protein response, is upregulated in the mouse cardiomyocyte cell line HL-1 when cultured under hypoxia. In vivo, in the left anterior artery descending (LAD) ligation mouse model of acute myocardial infarction, similar to PDI, PDIA6 protein expression was enhanced in the infarcted area (LAD+) relative to uninfarcted sham-tissue or the neighbouring area at risk (LAD-) of C57BL/6J mice. Interestingly, we found that ex-germ-free (ex-GF) mice subjected to the LAD ligation model for 24 hours had a reduced ejection fraction compared with their conventionally-raised (CONV-R) SPF controls. Furthermore, the LAD+ area in the infarcted heart of ex-GF mice showed reduced PDIA6 expression relative to CONV-R controls, suggesting that the presence of a gut microbiota enhanced LAD ligation-triggered PDIA6 expression. Collectively, our results demonstrate that PDIA6 is upregulated in cardiomyocytes as a consequence of hypoxia. In the LAD mouse model, PDIA6 was also increased in the infarcted area under in vivo conditions, but this increase was suppressed in ex-GF mice relative to CONV-R controls.

Introduction

Acute myocardial infarction (AMI) triggers the unfolded protein response (UPR) in cardiomyocytes to protect the ischemic surrounding from hypoxic stress (Thuerauf et al., 2006; Wang et al., 2018). PDI (P4HB), the prototypic PDI family member ensuring proper protein folding in the endoplasmatic reticulum, was previously shown to protect from myocardial infarction (Toldo et al., 2011a). However, there is an increase in P4HB levels with a paradoxical decrease of its active form in the infarcted diabetic mouse heart (Toldo et al., 2011b). PDI and other PDI family members are instrumental to ensure correct protein folding and to enhance superoxide dismutase 1 activity (Toldo et al., 2011a). Adenoviral transfection and overexpression of PDI in the mouse myocardium was shown to attenuate cardiac remodeling and to diminish cardiomyocyte apoptosis (Toldo et al., 2011a). Inside the vasculature, the oxidoreductase function of PDI is critical for the activation of cryptic blood-borne tissue factor on monocytes, the coagulation initiator that promotes arterial thrombus formation (Reinhardt et al., 2008). Furthermore, the oxidoreductase PDI regulates fibrin-mediated platelet aggregation (Lahav et al., 2002). PDI expression was also elevated in the myocardium of mice that were exposed to systemic hypoxia and in infarcted heart tissue (Tian et al., 2009). In addition to cardiomyocytes, the expression of P4HB, which protects from apoptosis and promotes cell migration and adhesion, is also induced in endothelial cells (Tian et al., 2009). Hence, it is relevant to explore whether other PDI family members that are involved in the setting of acute myocardial infarction, are induced in cardiomyocytes.

In mammalian cells, three distinct pathways regulate the UPR: ER transmembrane inositol-requiring enzyme 1 α (IRE1 α), pancreatic ER kinase (PERK), and activating transcription factor 6 (ATF6). Hypoxia is a well-recognized activator of the UPR in cardiac myocytes (Thuerauf et al., 2006). The PDI family member PDIA6 (ERP5,

TXNDC7) is an endoplasmic reticulum (ER) resident protein that plays a crucial role in ER stress, as it limits the activation of the UPR by blocking the activity of the UPR sensor IRE1 α through its direct binding to cysteine 148 and also acts on PERK (Eletto et al., 2014). An additional pool of PDIA6 acts as a cofactor of binding immunoglobulin protein (BiP; GRP-78), an ER resident chaperone (Jessop et al., 2009). Interestingly, the loss of PDIA6 does not result in ER stress and impaired protein folding (Rutkevich et al., 2010), but vice versa, it has been demonstrated with neonatal rat ventricular myocytes that the PDIA6 underlies regulation by ATF6, which is activated by hypoxia and that adenoviral overexpression of PDIA6 protects cardiomyocytes from stimulated ischemia/reperfusion-induced cell death (Vekich et al., 2012; Doroudgar et al., 2009).

Interestingly, recent research has revealed that impairment of the ER stress response in the gut epithelium is linked to intestinal dysbiosis and inflammation (Coleman et al., 2018; Kaser et al., 2008; Adolph et al., 2013), but it is currently unresolved whether the absence of a gut microbiota can impact the UPR in the intestine and whether hypoxia-regulated elements of the UPR are influenced by microbial colonization at remote vascular sites, such as the myocardium. As an improved ER-protein folding capacity supports cardiomyocyte survival and PDIA6 plays a protective role by limiting the UPR, it is crucial to understand the conditions that determine hypoxia-induced PDIA6 expression in cardiomyocytes.

Because the influence of hypoxia on PDIA6, as it occurs during acute myocardial infarction (AMI), is unexplored, we here studied the impact of hypoxia (1% oxygen) on the expression of PDIA6 in HL-1 cardiomyocytes. To analyse whether this UPR-regulator is influenced at the site of infarction in vivo, we analysed PDIA6 expression in a mouse model of AMI. Our results revealed that PDIA6 is upregulated in hypoxia-treated cardiomyocytes and in the infarcted cardiac tissue of LAD ligated mice. By

analyzing germ-free mice that were subjected to LAD ligation, we observed that the increase in PDIA6 expression in the murine myocardium was significantly reduced when the gut microbiota was absent, providing first evidence that the colonization status of the host may impact the UPR in the infarcted myocardium.

Results

Hypoxia increases the expression of PDIA6 in cultured HL-1 cardiomyocytes

Since PDIA6 has been suggested to be part of the ER stress response in cardiomyocytes, we used a hypoxic chamber to apply 1% hypoxia for 12 and 24 hours to cultured HL-1 cells (Claycomb et al., 1998). We confirmed the hypoxic conditions by the expected upregulation of hypoxia-inducible factor-1- α (HIF1 α) after 24 hours of incubation (**Fig. 1A**), which escapes degradation due to the absence of PHD mediated hydroxylation under hypoxic conditions (**Fig. S1**) (Hölscher et al., 2011; Myllyharju J, 2008). Strikingly, in addition to PDI (P4HB), our experiments comparing hypoxic HL-1 cardiomyocytes revealed that the protein levels of PDIA6 are likewise increased during hypoxia after 12 hours (**Fig. 1B, C**). In contrast, at 24 hours of incubation only a tendency of increased PDIA6 expression was detected (not shown). In contrast, this increase in PDIA6 protein levels was not detected in human umbilical vein endothelial cells (HUVECs) (**Fig. S2**). Therefore, our results demonstrate that PDIA6, which was previously identified as a negative regulator of the unfolded protein response (Eletto et al., 2014), is increased by hypoxia in cultured cardiomyocytes.

Expression of PDIA6 is enhanced in the infarcted mouse myocardium

We next interrogated whether PDIA6 protein levels are also upregulated in the infarcted tissue area applying the LAD ligation mouse model of acute myocardial infarction. Infarction was confirmed by ultrasound imaging, indicated by a significant reduction of the left ventricular ejection fraction 24 hours post LAD ligation (**Fig. 2A**). This model causes hypoxic conditions in the infarcted area (LAD+), since hypoxia-regulated gene expression is elevated relative to sham tissue or the neighbouring area at risk (LAD-), as confirmed by elevated PHD3 expression levels (**Fig. 2B**) (Hirsilä M, 2003; Rohrbach S, *Biogerontology*, 2005). Similar to the established role of PDI (P4HB) (Toldo et al., 2011a), the UPR regulator PDIA6 was increased in the infarcted LAD+ area relative to the LAD- area or tissues taken from the same site of sham-operated mice (**Fig. 2C**). In accordance, PDI showed enhanced protein levels in the LAD+ and LAD- area relative to the tissues of sham-operated mice (**Fig. 2D**). This increase was further reflected by increased plasma PDI levels (**Fig. 2E**). Interestingly, PDIA6 protein levels were three-fold increased in the LAD+ area relative to specimens from sham-treated mice and PDIA6 was significantly increased in the LAD+ area compared to the LAD- area (**Fig. 2F**). The increase of PDI and PDIA6 in the infarcted myocardium was further corroborated by immunohistochemistry of LAD+ specimens relative to sham-operated control tissue (**Fig. 2G**). In line with PDI, our results indicate that the hypoxia-dependent increase of PDIA6 found in HL-1 cardiomyocytes can be translated to the experimental conditions of acute myocardial infarction, where the arterial supply of oxygen is ceased in the infarcted LAD+ area.

The gut microbiota determines the reduction in the ejection fraction and PDIA6 expression levels of the infarcted mouse heart

Since there is increasing evidence for the gut microbiota as a determinant of myocardial infarction (Lam et al., 2012) and since we found that the presence of a gut microbiota enhances angiotensin II-induced cardiac fibrosis (Karbach et al., 2016), we took advantage of the germ-free (GF) mouse model to explore whether the host colonization status impacts on ventricular function and myocardial PDI expression under ischemic conditions in the LAD ligation model. Effective myocardial infarction was induced by LAD ligation in the germ-free mice, as demonstrated by ultrasound imaging of the left ventricle (**Fig. 3A**). Interestingly, the sham-operated ex-GF mice had a significantly reduced ejection fraction as compared to conventionally-raised (CONV-R) controls (**Fig. 3B**). Intriguingly, we found a pronounced decrease of the ejection fraction in LAD ligated ex-GF mice after we normalized to sham-operated ex-GF mice as compared to the normalized LAD ligated CONV-R mice (**Fig. 3C**). As expected, also in the ex-GF mice, PDI and PDIA6 mRNA expression levels were increased in the LAD+ area relative to the LAD- area or sham-operated tissues of ex-GF mice that lack colonization with a gut microbiota (**Fig. 3D**). In the left ventricle, PDI and PDIA6 transcript levels were unchanged under basal conditions, comparing sham-operated CONV-R and ex-GF mice (**Fig. 3E**). Most interestingly, when we compared the PDIA6 transcript levels in the LAD+ area of ex-GF mice with those of CONV-R mice, we noted a significantly reduced PDIA6 expression in response to LAD ligation (**Fig. 3F**). This is in contrast to the transcript levels of PDI, which were unchanged in the LAD+ area between ex-GF and CONV-R mice (**Fig. 3F**). Hence, our results imply that the presence of a gut microbiota, which acts as a chronic inflammatory stimulus, can affect the LAD ligation-induced UPR in the mouse myocardium.

Discussion

Our results show a direct upregulation of PDIA6 in cardiomyocytes due to hypoxic culture conditions. The *in vivo* relevance of increased PDIA6 in cardiomyocytes, an established regulator of the UPR, was further demonstrated under conditions of AMI in the murine model of myocardial infarction (permanent LAD ligation). Intriguingly, we found that the LAD-ligation-induced upregulation of PDIA6 was significantly reduced in the LAD+ area of ex-germ-free mice relative to their conventionally-raised counterparts, providing first evidence that the UPR of the infarcted heart may be influenced by the colonization status of the host.

In contrast to previous studies that identified PDIA6 in isolated rat cardiac myocytes, demonstrating the regulation via ATF6 and as an integral part of the ER stress response (Vekich et al., 2012; Eletto et al., 2014), we could for the first time demonstrate that hypoxia (1% oxygen) induced increased expression of this UPR-regulating factor in the HL-1 cardiomyocyte cell line. This finding is in line with the hypoxia-dependent upregulation of PDIA6 reported in a human cervix cancer cell line (SiHa) and a human head and neck cancer cell line (FaDu_{DD}) (Sørensen et al., 2009). This indicates that the hypoxia dependent upregulation of PDIA6 is not restricted to cardiac myocytes. Remarkably, because hypoxia-induced ATF6 upregulation protects rats from ischemia/reperfusion-induced necrosis (Jia et al., 2016) and PDIA6 is induced by ATF6 in ischemia/reperfusion and has a protective role in cardiomyocytes (Vekich et al., 2012), our results with HL-1 cells cultured at 1% oxygen atmosphere in a hypoxic chamber imply that PDIA6 mediates part of this protective hypoxia-dependent effect.

Hypoxia evokes the UPR in the ER, as shown in ventricular myocyte cultures (Thuerlauf et al., 2006). To explore whether PDIA6 is a relevant hypoxia-regulated factor during AMI, we have tested the *in vivo* relevance of the identified hypoxia-induced PDIA6 upregulation, which is specific to cardiomyocytes in the mouse model of myocardial infarction by permanent LAD ligation, showing a vast increase of PDIA6 protein expression in the infarcted LAD+ area, but not in the LAD- area (area at risk). This is in contrast to prototypic PDI, which was also increased in the LAD- area. In a seminal study with adenoviral constructs that either increased or suppressed PDIA6 expression, it has been convincingly demonstrated that PDIA6 protects neonatal rat ventricular myocytes from stimulated ischemia/reperfusion-induced cell death (Vekich et al., 2012). Furthermore, previous molecular biological studies have revealed that hypoxia-dependent ATF6 promotes PDIA6 expression (Vekich et al., 2012) and that PDIA6 controls the attenuation of IRE1 and PERK signals, but does not impact on ATF6 signaling (Eletto et al., 2014). Thus, our result on the upregulation of PDIA6 in infarcted heart tissue is coherent with the established role of PDIA6 in attenuating the hypoxia-induced UPR that was identified in cell culture models.

The gut microbial ecosystem influences vascular physiology and there is emerging evidence for the implication of the gut microbiota as a determinant of the extent of myocardial infarction (Reinhardt C et al., 2012; Lam et al., 2012; Lam et al., 2016). In previous work, we have identified that the colonization status of the host impacts angiotensin II-triggered cardiac fibrosis and tissue infiltration with myeloid cells (Karbach et al., 2016). Therefore, we applied the LAD ligation model to ex-germ-free mice to study the extent of the functional impairment of ventricular function in gnotobiotic mice and to test whether the expression of UPR regulator PDIA6 is influenced by the absence of the gut microbiota. With ex-GF mice, we revealed that

in the absence of the gut microbiota, the LAD ligation-induced increase of PDIA6, which suppresses the UPR in the ER, is severely perturbed. This was associated with an increased drop of the ejection fraction in ex-GF mice relative to CONV-R controls at 24 hours of LAD ligation-induced myocardial infarction. Of note, there is still no remodelling at this early time point. As the upregulation of PDIA6 protects neonatal rat ventricular cardiomyocytes from simulated ischemia/reoxygenation-induced cell death (Vekich et al., 2012), it is conceivable that the impaired cardiovascular function following LAD ligation in the ex-GF mouse model relative to conventionally-reared controls is due to the reduced upregulation of PDIA6 as part of the myocardial UPR. Additional work with gnotobiotic mouse models is required to define the role of colonizing microbial communities in myeloid cell infiltration and cardiac remodelling during AMI. As the loss of PDIA6 does not result in significant ER stress and impaired protein folding (Rutkevich et al., 2010), it will be important to target PDIA6 in an in vivo mouse model of AMI to explore how this hypoxia-induced UPR regulator affects infarct size. Future studies should also delineate the exact pathways of the ER stress response that are regulated by the deficiency or increased activity of PDIA6 in AMI.

Materials and Methods

Animals. C57BL/6J mice were 8–14 weeks old male mice housed in the Translational Animal Research Center (TARC) of the University Medical Center Mainz under specific pathogen free (SPF) or germ-free (GF) conditions in EU type II cages with 2-5 cage companions with standard autoclaved lab diet and water ad libitum, $22 \pm 2^\circ\text{C}$ room temperature and a 12 h light/dark cycle. GF mice were maintained as a GF mouse colony in sterile flexible film mouse isolator systems. The germ-free status of mice was tested weekly by PCR for detection of 16S rDNA and

by bacterial culture. GF mice, named as ex-GF, were kept under standard SPF conditions following LAD ligation for 24 hours. All groups of mice were age and weight-matched and were free of clinical symptoms. All procedures performed on mice were approved by the local committee on legislation on protection of animals (Landesuntersuchungsamt Rheinland-Pfalz, Koblenz, Germany; G10-1-051).

Cell culture. The HL-1 cell line, derivatives from the AT-1 mouse atrial cardiomyocyte tumor lineage (Claycomb et al., 1998), was maintained in Claycomb medium (Sigma, St. Louis, MI) supplemented with 0,1 mM Norepineprin, 2 mM L-glutamine, 100 U/ml penicillin/streptomycin and 10% v/v fetal bovine serum. Cells were seeded in 6-well plates, coated overnight with 0.02% w/v gelatin and 0.5% v/v fibronectin. Upon 80% confluency or more, cells were placed in the hypoxic chamber adjusted at 1% O₂ and 5% CO₂, at 37°C (Coy Laboratory Products Inc., Grass Lake, MI), they were washed and supplemented with hypoxic Claycomb medium and they were incubated for 12 or 24 hours in hypoxia or normoxia. After the desired time point, cells were washed and lysed for RNA or protein extraction.

Left anterior descending coronary artery ligation. Male mice (8 to 12 week old) underwent either permanent left anterior decenting (LAD) ligation injury or sham operation. Mice were anesthetized through intraperitoneal injection of midazolam (5 mg/kg BW) and medetomidine (0.5 mg/kg BW) and fentanyl (0.05 mg/kg BW). During surgery, mice are mechanically ventilated using a rodent ventilator. Ischemia injury was induced by permanent occlusion of the LAD artery with a 8-0 prelene suture (Johnson & Johnson Medical GmbH Ethicon, Germany). The ischemic area below ligation was reassured by visual examination of a bright color in the occluded myocardium. Atipamezol (0.05 mg/kg BW) and flumazenil (0.01 ml/kg BW) were

administered to the mice for analgesia after operation. Sham mice underwent the same operation procedure except coronary artery ligation. Mice were sacrificed 24h after ligation by exsanguination in isoflurane anesthesia.

Ultrasound imaging. Mice were anesthetized with isoflurane, heart rate and temperature were monitored during examination. High frequency ultrasound was performed by Vevo 770 system (FUJIFILM, VisualSonics, Toronto, Canada) represented as Ejection Fraction (EF%). Images were obtained from the left parasternal-long axis and short axis. In a two dimensional guided m-mode (2D), various parameters including left ventricular end-diastolic diameter (LVEDD) and left ventricular end systolic diameter (LVESD) were measured in accordance with American Society of Echocardiography.

Preparation of protein extracts from cells or tissues. Samples were mechanically lysed in cell lysis buffer (50mM Tris-HCl, 150mM NaCl, 5mM EDTA, 1% Triton X-100, pH 8) containing complete protease inhibitor cocktail tablets (Roche, Penzberg, Germany), passing through a 30Gx1/2" needle at least five times. The homogenates were incubated for 30 min on ice and centrifuged 3 times at 9.000 x g for 10 min at 4°C to remove insoluble debris. Tissues were homogenised in cell lysis buffer by the Tissue Lyser II (Qiagen, Hilden Germany) for 5 min at 30Hz. They were then kept on ice for 30 min and centrifuged 3 times at 9.000 x g for 10 min at 4°C to remove insoluble debris. Protein concentrations for both cells and tissues were quantified using the DC Protein Assay Kit 2 (BioRad, Hercules, CA) according to manufacturer's instructions.

Western blot. Protein lysates were supplemented with 3x sample loading buffer (62.5 mM Tris-HCl pH 6.8, 2.5% w/v SDS, 0.002% w/v bromophenol blue, 5% v/v β -mercaptoethanol, 10% v/v glycerol) and the proteins were denatured for 10 min at 99 °C. 30 μ l of the denatured proteins were subjected to an 8% SDS-polyacrylamide gel electrophoresis and were then transferred onto a nitrocellulose membrane. Unspecific binding was blocked with 5% BSA in Tris buffered saline (TBS) supplemented with Tween 20 (20 mM Tris-base, 137 mM NaCl, 0.05% v/v Tween 20) for 30 min and the primary antibodies HIF-1-alpha, anti-P4Hb EPR9498, anti PDIA6, EPR11132 (abcam, Cambridge, UK), β -actin and α -actinin (cell signalling, Danvers, MA) were incubated overnight at 4 °C with 1:1000 dilution and with gentle agitation. The membrane was washed for 1 h with TBST buffer and the secondary antibody peroxidase anti-rabbit IgG (H+L), in 1:10.000 dilution (Vector Laboratories, Burlingame, CA) was incubated for 1 h. The membrane was washed for 1 h with TBST buffer and incubated in luminol chemiluminescent substrate (cell signalling, Danvers, MA) for 1 min. The membranes were developed by a Chemi Doc Touch imaging system (BioRad, CA) and the densitometry analysis was performed by using ImageJ software (<https://imagej.nih.gov/ij/>).

Quantitative real-time PCR. Total RNA was isolated from the cells with the RNeasy Kit and from the tissues with the RNeasy Fibrous Tissue Mini Kit (Qiagen, Hilden, Germany) according to manufacturer's instructions. Total RNA (2 μ g) was reverse transcribed with the High Capacity cDNA Reverse Transcription Kit (Applied Biosystems, Foster City, USA) and SYBR green-based qRT-PCR was performed with iQ SYBR Green Supermix (Bio-Rad Laboratories, Hercules, CA, USA). The oligonucleotide sequences used are listed in Table 1.

Target	Gene		Sequence 5' → 3'
Protein disulfide isomerase	P4HB	forward	CCGTGGCTACCCCACAATC
		reverse	GCAGTGTCAGACAGGGTTGTA
Protein disulfide isomerase family A member 6	PDIA6	forward	AGCTGCACCTTCTTTCTAGCA
		reverse	CAGGCCGTCACTCTGAATAAC
Hypoxia-Inducible Factor Prolyl Hydroxylase 2	EGLN1	forward	AGCTGGTCAGCCAGAAGAGT
		reverse	GCCCTCGATCCAGGTGATCT
Hypoxia-Inducible Factor Prolyl Hydroxylase 1	EGLN2	forward	AGTCCTTGGAGTCTAGCCGAAG
		reverse	TGGCAGTGGTCGTAGTAGCA
Hypoxia-Inducible Factor Prolyl Hydroxylase 3	EGLN3	forward	AGGCAARGGTGGCTTGCTATC
		reverse	GCGTCCCAATTCTTATTCAGGT
ribosomal protein L32	L32	forward	CCTCTGGTGAAGCCCAAGATC
		reverse	TCTGGGTTTCCGCCAGTTT

Mouse PDI (P4HB) and PDIA6 ELISA. ELISAs for both PDI and PDIA6 was performed according to manufacturer's instructions (MyBioSource.com, San Diego, CA).

Immunohistochemistry. Tissues were fixed in Roti[®]-Histofix 4% (Carl Roth GmbH + Co. KG, Karlsruhe, Germany) and provided to the Core Facility Histology of the University Medical Center Mainz for PDI with anti-P4Hb antibody (abcam, Cambridge, UK) and for PDIA6 (Aviva systems biology, San Diego, CA) staining. All sections were analyzed by light microscopy (Axia Lab.A1, Zeiss, Oberkochen, Germany).

Statistical analysis. All values are expressed as the mean \pm SEM. Data sets were analysed with GraphPad Prism 6 (GraphPad Software Inc., San Diego, USA) using one-way analysis of variance (ANOVA) or unpaired t-tests. Differences of $P < 0.05$ were considered statistically significant.

Acknowledgment: The authors state that no conflict of interests exists. We are grateful to Cornelia Karwot and Klaus-Peter Derreth for expert technical assistance. We thank Prof. William Claycomb and Dr. May L. Lam from the Department of Biochemistry and Molecular Biology at Louisiana State University Health Science Center, New Orleans for providing us with the HL-1 cell line. Author contributions: K.K. performed experiments, analysed and interpreted data and participated in manuscript writing. S.F. and V.S.G. performed experiments. W.C., M.L.L., and M.K. analysed data. U.W. and P.W. were involved in drafting the manuscript. C.R. designed experiments, analysed data, and wrote the manuscript.

Competing Interests: No competing interests declared.

Funding: The project was funded by the CTH Junior Group Translational Research in Thrombosis and Hemostasis (BMBF 01EO1003 and 01EO1503), DFG Individual Grant (RE 3450/3-1) and a project grant from the Boehringer Ingelheim Foundation to C.R.. K.K. was a fellow of the graduate school Translational Biomedicine (TransMed). U.W., P.W. and C.R. are members of DZHK.

References

Adolph, T.E., Tomczak, M.F., Niederreiter, L., Ko, H.J., Böck, J., Martinez-Naves, E., Glickman, J.N., Tschurtschenthaler, M., Hartwig, J., Hosomi, S., Flak, M.B., Cusick, J.L., Kohno, K., Iwawaki, T., Billmann-Born, S., Raine, T., Bharti, R., Lucius, R., Kweon, M.N., Marciniak, S.J., Choi, A., Hagen, S.J., Schreiber, S., Rosenstiel, P., Kaser, A. and Blumberg, R.S. (2013). Paneth cells as a site of origin for intestinal inflammation. *Nature* **503**, 272-276.

Claycomb, W.C., Lanson, N.A. Jr., Stallworth, B.S., Egeland, D.B., Delcarpio, J.B., Bahinski, A. and Izzo, N.J. Jr. (1998). HL-1 cells: a cardiac muscle cell line that contracts and retains phenotypic characteristics of the adult cardiomyocyte. *Proc. Natl. Acad. Sci. U.S.A.* **95**, 2979-2984.

Coleman, O.I., Lobner, E.M., Bierwirth, S., Sorbie, A., Waldschmitt, N., Rath, E., Berger, E., Lagkouravdos, I., Clavel, T., McKoy, K.D., Weber, A., Heikenwalder, M., Janssen, K.P. and Haller, D. (2018). Activated ATF6 induces intestinal dysbiosis and innate immune response to promote colorectal tumorigenesis. *Gastroenterology* doi: 10.1053/j.gastro.2018.07.028.

Doroudgar, S., Thuerlauf, D.J., Marcinko, M.C., Belmont, P.J. and Glembotski, C.C. (2009). Ischemia activates the ATF6 branch of the endoplasmic reticulum stress response. *J. Biol. Chem.* **284**, 29735-29745.

Eletto, D., Eletto, D., Dersh, D., Gidalevitz, T. and Argon, Y. (2014). Protein disulfide isomerase A6 controls the decay of IRE1 α signaling via disulfide-dependent association. *Mol. Cell.* **53**, 562-676.

Hirsilä, M., Koivunen, P., Günzler, V., Kivirikko, K.I. and Myllyharju J. (2003). Characterization of the human prolyl 4-hydroxylases that modify the hypoxia-inducible factor. *Biol. Chem.* **278**, 30772-30780.

Hölscher, M., Silter, M., Krull, S., von Ahlen, M., Hesse, A., Schwartz, P., Wielockx, P., Breier, G., Katschinski, D.M. and Zieseniss, A. (2011). Cardiomyocyte-specific prolyl-4-hydroxylase domain 2 knock out protects from acute myocardial injury. *J. Biol. Chem.* **286**, 11185-11194.

Jia, W., Jian, Z., Li, J., Luo, L., Zhao, L., Zhou, Y., Tang, F. and Xiao, Y. (2016). Upregulated ATF6 contributes to chronic intermittent hypoxia-afforded protection against myocardial ischemia/reperfusion injury. *Int. J. Mol. Med.* **37**, 1199-1208.

Jessop, C.E., Watkins, R.H., Simmons, J.J., Tasab, M. and Bulleid, N.J. (2009). Protein disulphide isomerase family members show distinct substrate specificity: P5 is targeted to BiP client proteins. *J. Cell. Sci.* **122**, 4287-4295.

Karbach, S.H., Schönfelder, T., Brandão, I., Wilms, E., Hörmann, N., Jäckel, S., Schüler, R., Finger, S., Knorr, M., Lagrange, J., Brandt, M., Waisman, A., Kossmann, S., Schäfer, K., Münzel, T., Reinhardt, C. and Wenzel, P. (2016). Gut microbiota promote angiotensin II-induced arterial hypertension and vascular dysfunction. *J. Am. Heart Assoc.* **5**, doi: 10.1161/JAHA.116.003698.

Kaser, A., Lee, A.H., Franke, A., Glickman, J.N., Zeissig, S., Tilg, H., Nieuwenhuis, E.E., Higgins, D.E., Schreiber, S., Glimcher, L.H. and Blumberg, R.S. (2008). XBP1 links ER stress to intestinal inflammation and confers genetic risk for human inflammatory bowel disease. *Cell* **134**, 743-756.

Lahav, J., Jurk, K., Hess, O., Barnes, M.J., Farndale, R.W., Luboshitz, J. and Kehrel, B. (2002). Sustained integrin ligation involves extracellular free sulfhydryls and enzymatically catalyzed disulfide exchange. *Blood* **100**, 2472-2478.

Lam, V., Su, J., Koprowski, S., Hsu, A., Tweddell, J.S., Rafiee, P., Gross, G.J., Salzman, N.H. and Baker, J.E. (2012). Intestinal microbiota determine severity of myocardial infarction in rats. *FASEB J.* **26**, 1727-1735.

Lam, V., Su, J., Hsu, A., Gross, G.J., Salzman, N.H. and Baker, J.E. Intestinal microbial metabolites are linked to severity of myocardial infarction in rats. *PLoS. One.* **11**, e0160840.

Myllyharju, J. (2008). Prolyl 4-hydroxylases, key enzymes in the synthesis of collagens and regulation of the response to hypoxia, and their roles as treatment targets. *Ann Med.* **40**, 402-417.

Reinhardt, C., von Brühl, M.-L., Manukyan, D., Grahl, L., Lorenz, M., Altmann, B., Dlugai, S., Hess, S., Konrad, I., Orschiedt, L., Mackman, N., Ruddock, L., Massberg, S. and Engelmann, B. (2008). Protein disulfide isomerase acts as an injury response signal that enhances fibrin generation via tissue factor activation. *J. Clin. Invest.* **118**, 1110-1122.

Reinhardt, C., Bergentall, M., Greiner, T.U., Schaffner, F., Östergren-Lundén, G., Petersen, L.C., Ruf, W. and Bäckhed, F. (2012). Tissue factor and PAR1 promote microbiota-induced intestinal vascular remodelling. *Nature* **483**, 627-631.

Rohrbach, S., Simm, A., Pregla, R., Franke, C. and Katschinski, D.M. (2005). Age-dependent increase of prolyl-4-hydroxylase domain (PHD) 3 expression in human and mouse heart. *Biogerontology* **6**, 165-171.

Rutkevich, L.A., Cohen-Doyle, M.F., Brockmeier, U. and Williams, D.B. (2010). Functional relationship between protein disulfide isomerase family members during the oxidative folding of human secretory proteins. *Mol. Biol. Cell.* **21**, 3093-3015.

Sørensen, B.S., Horsman, M.R., Vorum, H., Honoré, B., Overgaard, J. and Alsner, J. (2009). Proteins upregulated by mild and severe hypoxia in squamous cell carcinomas in vitro identified by proteomics. *Radiother. Oncol.* **92**, 443-449.

Thuerauf, D.J., Marcinko, M., Gude, N., Rubio, M., Sussman, M.A. and Glemotski, C.C. (2006). Activation of the unfolded protein response in infarcted mouse heart and hypoxic cultured cardiac myocytes. *Circ. Res.* **99**, 275-282.

Tian, F., Zhou, X., Wikström, J., Karlsson, H., Sjöland, H., Gan, L.M., Borén, J. and Akyürek, L.M. (2009). Protein disulfide isomerase increases in myocardial endothelial cells in mice exposed to chronic hypoxia: a stimulatory role in angiogenesis. *Am. J. Heart. Circ. Physiol.* **297**, H1078-1086.

Toldo, S., Severino, A., Abbate, A. and Baldi, A. (2011). The role of PDI as a survival factor in cardiomyocyte ischemia. *Methods. Enzymol.* **489**, 47-65.

Toldo, S., Boccellino, M., Rinaldi, B., Seropian, I.M., Mezzaroma, E., Severino, A., Quagliuolo, L., Van Tassell, B.W., Marfella, R., Paolisso, G., Rossi, F., Natarajan, R., Voelkel, N., Abbate, A., Crea, F. and Baldi, A. (2011). Altered oxidoreductive state in the diabetic heart: loss of cardioprotection due to protein disulfide isomerase. *Mol. Med.* **17**, 1012-1021.

Vekich, J.A., Belmont, P.J., Thuerauf, D.J. and Glemotski, C.C. (2012). Protein disulfide isomerase-associated 6 is an ATF6-inducible ER stress response protein that protects cardiac myocytes from ischemia/reperfusion-mediated cell death. *J. Mol. Cell. Cardiol.* **53**, 259-267.

Wang, X., Bi, X., Zhang, G., Deng, Y., Luo, X., Xu, L., Scherer, P.E., Ferdous, A., Fu, G., Gillette, T.G., Lee, A.S., Jiang, X. and Wang, Z.V. (2018). Glucose-regulated protein 78 is essential for cardiac myocyte survival. *Cell. Death. Differ.* doi: 10.1038/s414118-018-0109-4.

Figures

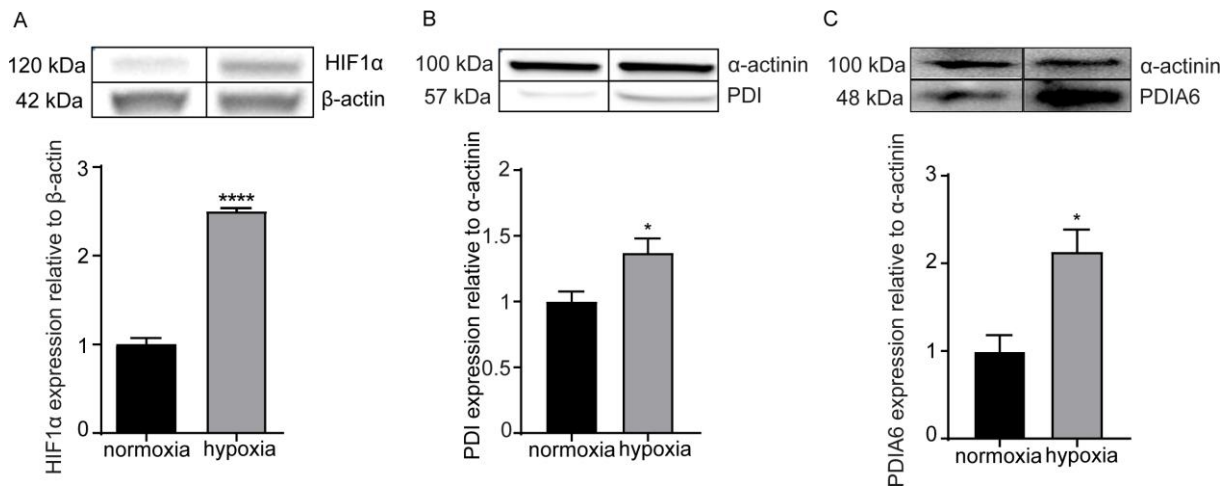


Fig. 1.

Hypoxia-induced upregulation of HIF1α, PDI and PDIA6 in HL-1 cardiomyocytic cells. (A) Hypoxia-dependent (1% O₂) increase in HIF1α protein expression relative to β-actin (n=3, 24h incubation). (B) Hypoxia-dependent (1% O₂) increase in PDI (n=4, 24h incubation) and (C) PDIA6 (n=3, 12h incubation) protein levels relative to α-actinin. Normoxia, black bar; hypoxia, grey bar. All data were expressed as the means ± SEM. Statistical comparisons were performed using the Student's *t*-test, * p < 0.05, ****p<0.0001.

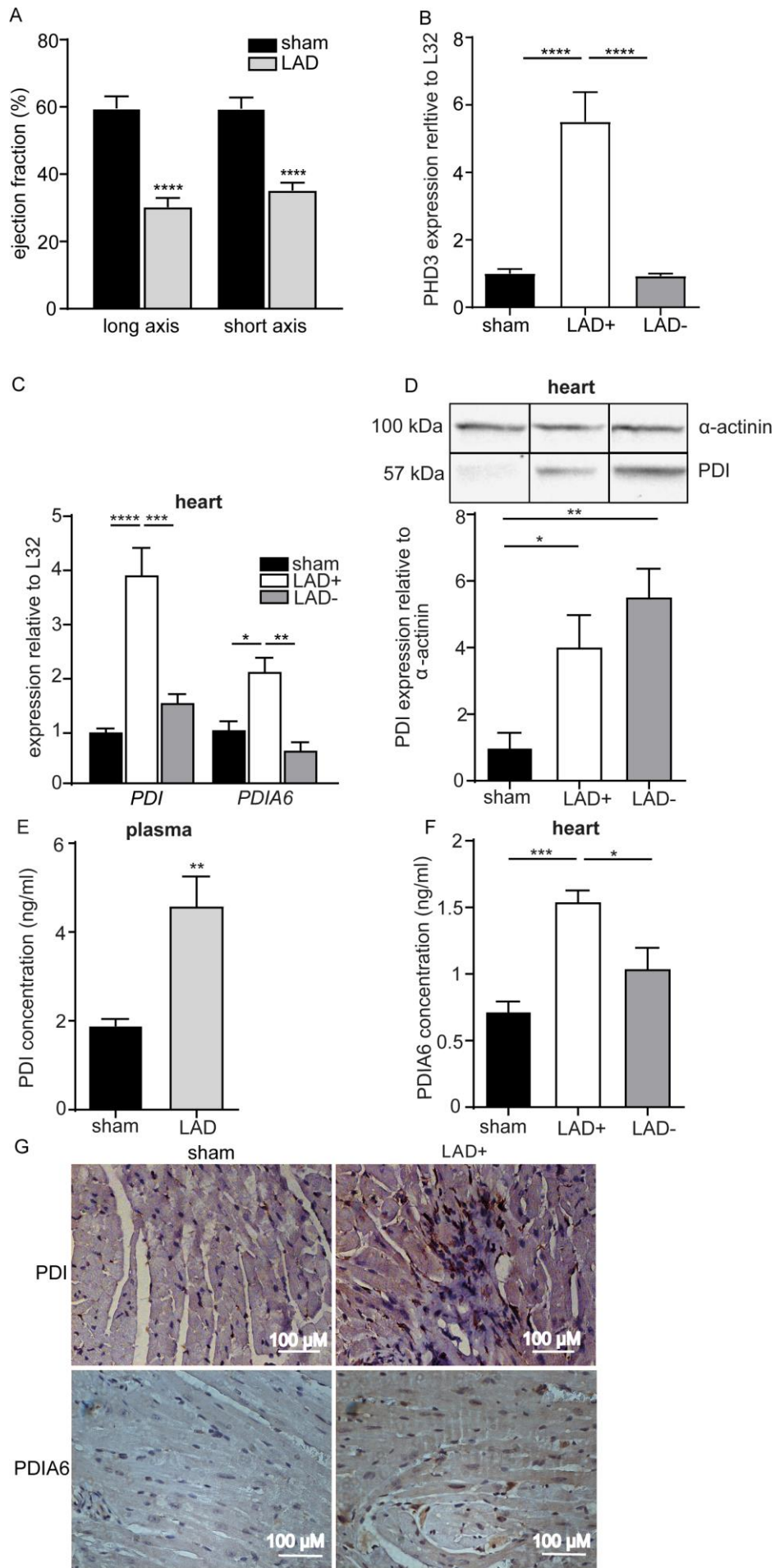


Fig.2.

The expression of PDI and PDIA6 is increased in the infarcted area (LAD+) in the 24 hours LAD ligation mouse model. (A) Long axis (n=6,9) and short axis (n=6,8) of the left ventricle after LAD ligation; SPF C57BL/6J mouse. (B) mRNA expression of the myocardial hypoxia marker PHD3 is increased relative to L32 in the LAD+ area compared with sham or LAD- tissues (n=4,5,5). (C) PDI and PDIA6 mRNA expression relative to L32 is increased in the LAD+ area compared with sham or LAD- tissues (n=5). (D) PDI protein levels are increased relative to α -actinin in the LAD+ (n=6) and LAD- (n=6) compared to sham-operated heart tissue (n=5) (Western blot) and (E) in plasma (ELISA) (n=6,8). (F) PDIA6 protein levels are increased in LAD+ heart tissue relative to sham or LAD- tissues (ELISA) (n=5). (G) Immunohistochemistry stainings for PDI (upper panel) and PDIA6 (lower panel) in sham-operated and infarcted LAD+ heart tissue (representative micrograph). Scale bar, 100 μ m. LAD+ represents the ligated areas, LAD- the area proximal to ligation and sham represents the sham-operated animals. All data were expressed as the means \pm SEM. Statistical comparisons were performed using the Student's *t*-test and one-way ANOVA, * $p < 0.05$, ** $p < 0.01$, *** $p < 0.001$, **** $p < 0.0001$.

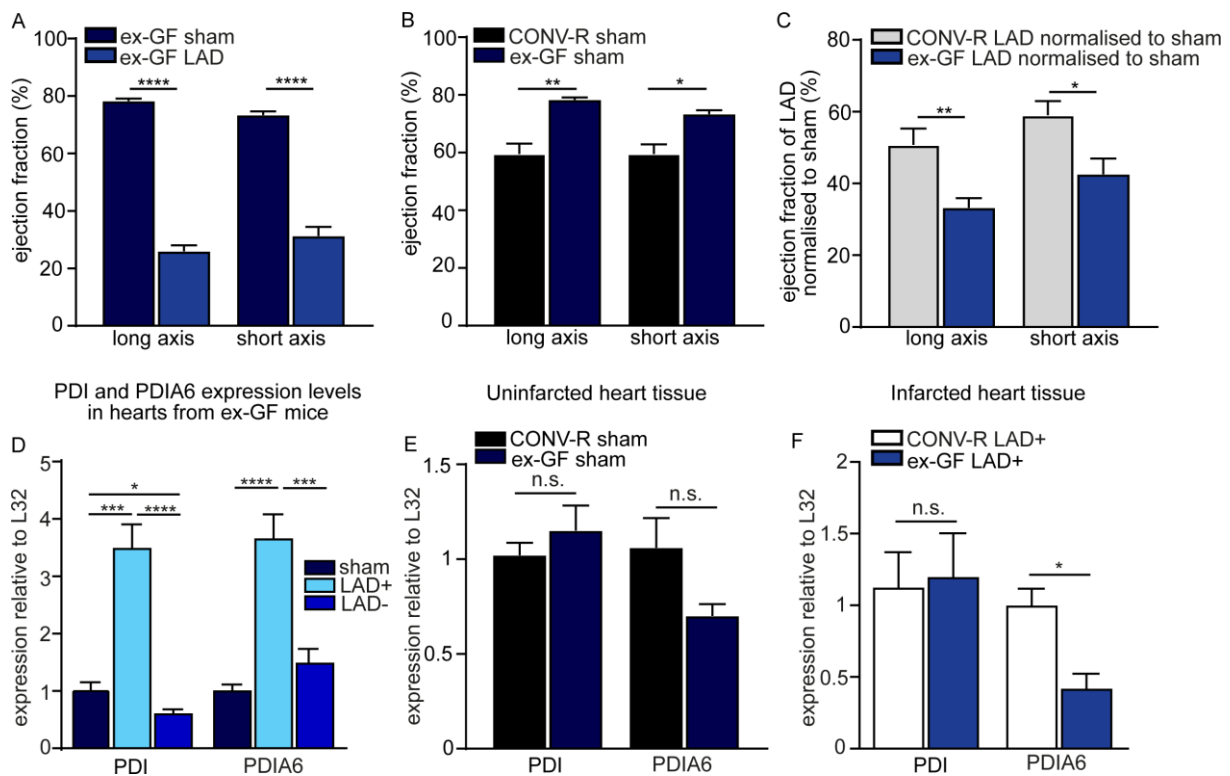
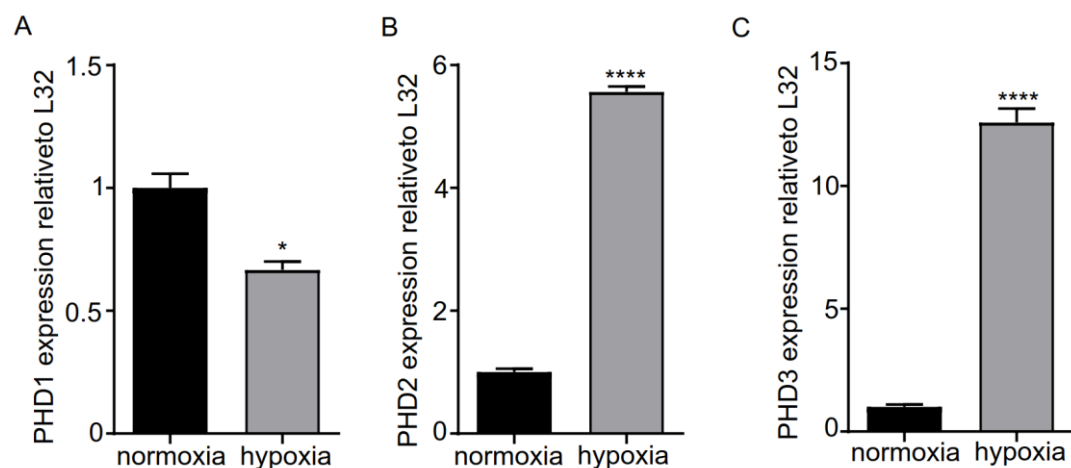


Fig. 3.

24 hours LAD ligation model of acute myocardial infarction on germ-free mice.

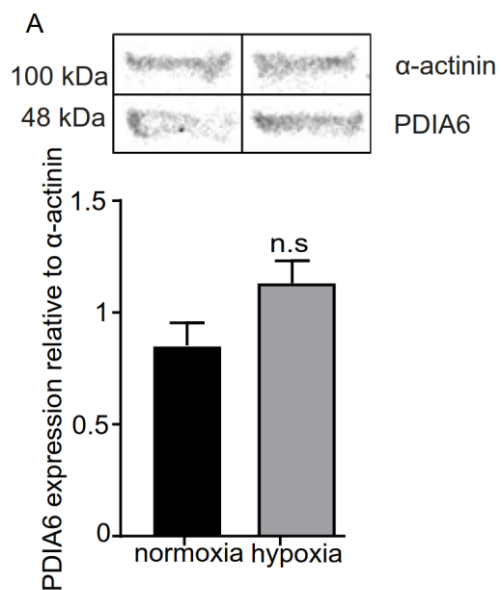
(A) Long axis (n=6,9) and short axis (n=6,8) of the left ventricle after LAD ligation of ex-germ-free (ex-GF) C57BL/6J mice as determined by ultrasound imaging. (B) Ejection fraction % of the long (n=6,3) and short axis (n=6,3) of sham-operated C57BL/6J mice kept under SPF conventionally-raised (CONV-R) or ex-GF conditions. (C) Comparison of the long axis (n=9,9) and the short axis (n=8,8) of CONV-R SPF C57BL/6J mice with ex-GF C57BL/6J mice normalized to sham-operated controls. (D) PDI (n=6,4,6) and PDIA6 (n=6,6,6) mRNA expression in sham-operated, LAD+ and LAD- heart tissues of ex-GF mice. (E) PDI and PDIA6 mRNA expression in heart tissues of sham-operated ex-GF mice compared to SPF CONV-R mice (n=6,3). (F) PDI (n=6) and PDIA6 (n=5) mRNA expression in LAD+ heart tissues of ex-GF mice compared to SPF CONV-R mice. LAD+ represents the ligated

area, LAD- the area proximal to ligation and sham represents the sham-operated animals. All data were expressed as the means \pm SEM. Statistical comparisons were performed using the Student's *t*-test or one-way ANOVA, n.s. not significant, * $p < 0.05$, *** $p < 0.001$, **** $p < 0.0001$.

Figure S1

HIF Prolyl Hydroxylase expression of the HL-1 cells in hypoxia. (A) PHD1 (n=3), (B) PHD2 (n=3) and (C) PHD3 (n=3) expression relative to L32 of the HL-1 cells incubated for 24h in normoxia or hypoxia (1% O₂). All data were expressed as the means \pm SEM. Statistical comparisons were performed using the Student's *t*-test * p<0.05, ****p<0.0001.

Figure S2



PDIA6 expression in HUVECs incubated in hypoxia. A. HUVECs incubated in normoxia or hypoxia (1% O₂) for 24h. Data were expressed as the means \pm SEM. Statistical comparisons were performed using the Student's *t*-test.